Mon. Not. R. astr. Soc. (1979) **186**, 799–812

Tidal torques on accretion discs in binary systems with extreme mass ratios

D. N. C. Lin and J. Papaloizou *Institute of Astronomy, University of Cambridge, Madingley Road, Cambridge CB3 0HA*

Received 1978 August 29; in original form 1978 July 6

Summary. This paper investigates the tidal transport of angular momentum in accretion disc flow in a close binary system with small mass ratio, q. We demonstrate that the disc can only be tidally truncated if q is greater than the inverse of the Reynolds number. We derive the existence of a strong 2:1 resonance. Near the resonance, a spiral dissipation pattern is expected. If the Reynolds number is greater than $\sim q^{-2}$, a dissipation and angular momentum loss from the disc may be sufficient to truncate it at the resonance. Finally we discuss the application of these results to dwarf novae.

1 Introduction

In this paper we consider the effect of the tidal force due to the secondary on an accretion disc around the primary in an interacting close binary system. Previous simulations and analytic calculations have shown that the tidal force can have a strong influence on the gas flow in the vicinity of the Roche lobe (Lin & Pringle 1976; Papaloizou & Pringle 1977). If the mass ratio q is of order unity, the tidal force effectively transports angular momentum between the gas and the binary orbit. As this occurs the fluid dissipates a large fraction of its kinetic energy in one orbital period.

In this paper we investigate tidal transport in the limit of a small mass ratio when the tidal force is weak. In Section 2 we derive the rate of tidal angular momentum transport in the context of mass transfer flow from a small star, the secondary, on to its massive companion, the primary. We show that in some cases the tidal force is too weak to compete with the viscous process. We discuss the implications for the evolution of dwarf novae systems. In Section 3 we demonstrate the presence of a strong resonance in the small q binary systems. We show that this resonance may have a significant effect in transferring angular momentum and produces a spiral dissipation pattern in the accretion disc flow around the primary. In Section 4 we discuss possible observational consequences of the results derived in this paper.

2 Tidal transport in close binary systems with small q

In this section we consider the tidal force due to a small companion on the gas flow around the massive primary star. When q is small, the tidal force of the secondary can only be felt during the phase when the particles have a close approach with the secondary. The amoun of angular momentum transferred between a particle and the binary orbit during such a clos encounter can be determined by a simple scattering calculation. As a particle passes by th secondary, the tidal force would deflect the orbit by a small angle such that

$$\cot^2(\delta/2) = u^4 a^2/G^2 m_2^2 \qquad (1$$

where u is the relative velocity and a is the impact parameter. Since only those particles a the outer edge of the disc will be affected by close encounters, the corresponding angula momentum per unit mass transferred would be

$$\Delta h = u(1 - \cos\delta) R \qquad (2$$

where R is the binary separation.

If the particles are circulating around the primary with an angular frequency Ω and th binary period is $2\pi/\omega$ we deduce $u = (\Omega - \omega) R$ and

$$\Delta h = 2G^2 m_2^2/[R^2(\Omega - \omega)^3 a^2]. \qquad (3$$

Since the time between encounters is $2\pi/(\Omega - \omega)$, the rate of specific angular momentur transfer would be

$$\dot{h} = G^2 m_2^2/[\pi R^2 a^2 (\Omega - \omega)^2]. \qquad (4$$

Using Taylor's expansion on Ω, we can deduce the rate of total angular momentur transport over the entire disc to be

$$\dot{H} = \frac{2G^2 m_2^2 R \Sigma}{R^2 (d\Omega/dR)^2} \int_A^\infty \frac{da}{a^4} = \frac{2G^2 m_2^2 \Sigma}{3RA^3 (d\Omega/dR)^2} \qquad (5$$

where Σ is the surface density and A is the minimum value of a. A can be taken to b the Roche radius of the secondary r_L. For small q, $r_L = R(q/3)^{1/3}$. The time-scale fo removing a large fraction of the angular momentum from the disc would be

$$\tau_{\text{tidal}} = \frac{\pi R^4 \Sigma \Omega}{\dot{H}} = \frac{27\pi}{8} \left(\frac{A}{R}\right)^3 \frac{1}{\Omega q^2} \frac{9\pi}{8q\Omega}. \qquad (6$$

This result can also be obtained by a more sophisticated perturbation analysis of the particl orbits around the primary (see Appendix A). In this treatment we assume that energy an angular momentum are only transferred by the tides during the phase of close approach c particles on initially circular orbits. Since the Jacobi constant $\epsilon - \omega h$, cannot be altered b tides, particles in an accretion disc inside the Roche lobe of the primary always lose angula momentum faster than energy. Consequently, their initially circular orbits become eccentri After the close encounter the tidal forces become very weak. If the viscous force is suff ciently strong, it will transfer angular momentum amongst the particles in order to achieve lower energy state (Lynden-Bell & Pringle 1974) and thereby recircularize the orbits. In th limit of small q our results should provide us with a slightly overestimated angular momer tum transport, as initially circular orbits are the most favourable.

In the region sufficiently near the primary, gas flow will be predominantly governed b the viscous process since the tidal force will be too weak to compete. Here the viscous forc transports angular momentum outwards to allow matter to fall inwards. In the process c redistributing angular momentum, kinetic energy of the fluid will be dissipated into heat an hence provide an energy source (Lynden-Bell & Pringle 1974). Such a source of energy believed to power the galactic X-ray binary sources and dwarf novae systems.

In the viscously dominated regions the time-scale for angular momentum transport is

$$\tau_{\text{visc}} = \mathscr{R}\Omega^{-1} \tag{7}$$

where $\mathscr{R}$ is the effective Reynolds number of the outer part of the disc.

Consider now the flow in the accretion disc. In order to accrete a small amount of matter from the disc near to the primary, roughly the same amount of matter must move to larger radii to absorb the angular momentum. Such transport will continue until all the angular momentum is dumped at the outer edge of the disc. At the outer edge, if τ_{visc} is still small compared with τ_{tidal} (i.e. $q < \mathscr{R}^{-1}$), the overall size of the disc would increase. However, if $q > \mathscr{R}^{-1}$, the tidal force is more efficient there, i.e. $t_{\text{tidal}} < t_{\text{visc}}$, the expansion can stop and the excess angular momentum can be transported to the binary orbit via the tidal torque. The tidal force would then truncate the disc.

The implications of our result for the evolution of mass transferring close binary systems is that when the mass ratio of the system is reduced to less than $\mathscr{R}^{-1}$, the tidal effect cannot stop the disc from expanding beyond the Roche lobe of the primary. Consequently, a significant fraction of the mass transferred from the secondary to the primary via the inner Lagrangian point will return to the secondary and in so doing reduces the effective mass transfer rate. This implies that it would be very difficult to reduce the mass ratio much below $\mathscr{R}^{-1}$.

To demonstrate this point we ran several numerical simulations. The numerical method we adopted has already been discussed in our previous work (Lin & Pringle 1976). We started the simulation by transferring matter at a constant rate from the secondary to the primary via the inner Lagrangian point. After 20 orbital periods or so we achieved a steady state. We then calculated the fractions of material transferred that were accreted by the primary, returned to the secondary, and lost from the system. These results are presented in Table 1. In these simulations the same viscosity is used but the mass ratio varied. In all cases a negligible fraction is lost from the system. In case one, q is chosen to be greater than $\mathscr{R}^{-1}$. The tidal force not only truncated the disc but also enabled about 90 per cent of the transferred material to be accreted by the primary. In case three, q is chosen to be less than $\mathscr{R}^{-1}$. The tidal force was unable to perturb the flow markedly and about 70 per cent of the transferred material actually returned to the secondary.

Table 1. f is that fraction of material transfer from the secondary to the primary via the Lagrangian point to be returned to the secondary. When the tidal force is dominant f is small. Most of the transferred material is returned to the secondary when the tidal force is weak.

q	$\mathscr{R}$	f	Remark
0.1	500	0.10	Disc truncated tidally with sharp edge
0.02	500	0.66	Disc marginally truncated with fuzzy edge
0.001	500	0.74	Disc not truncated and extended beyond Roche lobe

In reality, the magnitude of the Reynolds number is unknown. If one adopts the molecular viscosity, it would be of order 10^{14}. On the other hand if the flow in the disc is turbulent, it may be of order 10^{2-3} (Lynden-Bell & Pringle 1974). If we can observe a system with a small star transferring mass to a more massive star, the mass ratio may lead us to new information on the effective Reynolds number of the outer part of the disc.

3 The effect of the 2:1 resonance

Another interesting situation that may arise in gas flow in close binary systems is the presence of strong resonances. These resonances occur in regions of the disc where the

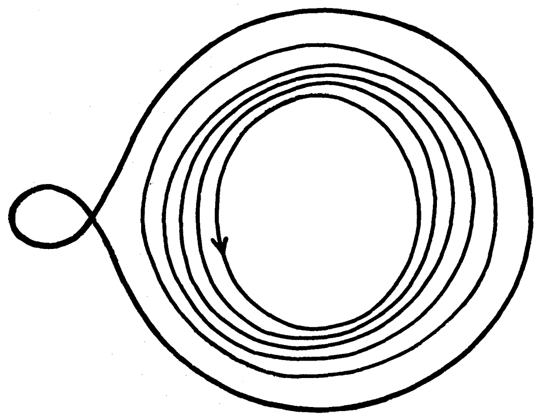

Figure 1. Schematic drawing of particle orbits around the 2:1 resonance for a binary system with $q = 50$.

particle angular frequency Ω is related to ω by $\Omega = n\omega/(n-1)$, for n integral (Papaloizou & Pringle 1977). In this section we consider the case $n = 2$. Due to the tidal influence of the secondary, the simply periodic orbits around the primary will be slightly elongated along either the binary axis or the axis perpendicular to it. At the resonant radius, the major axis of the simply periodic orbits undergoes a 90° rotation.

In a fluid disc, the viscous effect would smear out the transition (Lynden-Bell 1975), see Fig. 1. In the transition zone the flow converges at some orbital phases and diverges at other phases. This flow pattern would produce non-axisymmetric shear and lead to a spiral dissipation pattern. Such a pattern has been simulated in the context of bar driven spiral galaxies (Sanders & Huntley 1977).

Near the resonant radius, the accumulated tidal effect can also lead to efficient angular momentum transport (Lynden-Bell & Kalnajs 1972). The rate of resonant angular momentum transport has been calculated in the case of Saturn's rings (Goldreich & Tremaine 1978a) and spiral galaxies (Donner, private communication; Goldreich & Tremaine 1978b).

In the case of mass transfer and accretion disc flow we are primarily interested in the case when the resonant region is viscously dominated. We deduce the efficiency of angular momentum transfer near the resonance in this case, which is different from that considered in other investigations. Finally we note that the spiral dissipation pattern may lead to interesting effects on the light curves of some dwarf novae systems.

In an accretion disc around the primary star of a binary system, not all the resonances can be found. If the mass ratio is small, $\Omega = (R/r)^{3/2}\,\omega$, at radius r. Furthermore the Roche radius of the primary is $r_\mathrm{p} = R\{1 - (q/3)^{1/3}\}$. In order for a resonance with $\omega/\Omega = (n-1)/n$ to fall inside the Roche lobe of the primary, $r_n < r_\mathrm{p}$, or $q < 3[1 - (n-1)/n)^{2/3}]^3$. For most binary systems with q of order unity no resonance can be found inside the Roche lobe. However, for $q \lesssim 0.1$ a strong 2:1 (i.e. $n = 2$) resonance can fall inside the Roche lobe and in the disc. We demonstrate below both analytically and numerically that the 2:1 resonance can be strong enough to produce observable features.

To simplify the problem we shall treat the fluid in the disc to be isothermal and viscous with arbitrary amounts of bulk and shear viscosity. The effect of the secondary may be investigated by a perturbation analysis (Papaloizou & Pringle 1977) and the flow may be solved in terms of the Fourier component of the perturbed velocities u_r' and u_θ' such that

$$(u_{rm}', u_{\theta m}') = \int_0^{2\pi} (u_r', u_\theta') \exp\,[im(\theta - \omega t)]\, d\theta. \qquad (8)$$

Ignoring the zeroth-order radial velocity in the unperturbed flow, the perturbed equations of motion become

$$i(\Omega-\omega)\,mu'_{rm}-2\Omega u'_{\theta m}=-\frac{1}{\rho}\frac{\partial p'_m}{\partial r}-\frac{\partial \Psi'_m}{\partial r}+F_{\nu r} \tag{9}$$

$$i(\Omega-\omega)\,mu'_{\theta m}+\frac{\Omega}{r}u'_{rm}=-\left[\frac{p'_m}{\rho r}+\frac{\Psi'_m}{r}\right]+F_{\nu\theta} \tag{10}$$

where p'_m is the Fourier component of the perturbed pressure, ρ the mean flow density and $F_{\nu r}, F_{\nu\theta}$ are components of the viscous force.

Since we are interested only in a narrow region in the vicinity of the resonance all the terms except those with the highest radial derivatives in $F_{\nu r}$ and $F_{\nu\theta}$ are negligible, so that

$$F_{\nu r}=\left(\frac{4\nu}{3}+\xi\right)\frac{d^2u_{mr}}{dr^2}\quad\text{and}\quad F_{\nu\theta}=\frac{\nu\, d^2u_{m\theta}}{dr^2} \tag{11}$$

where ν and ξ are the shear and bulk viscosities. We note that the zeroth-order radial velocity would only be found in terms with lower derivatives and accordingly our earlier omission of these is justified. From the continuity equation we find

$$\rho'=\frac{i\rho\,\nabla\cdot\mathbf{u}'}{(\Omega-\omega)\,m}. \tag{12}$$

By introducing an isothermal equation of state $p'=\rho'c^2$ we can now solve all the equations (see Appendix B). The radial velocity at a distance x from the resonance is

$$u'_{mr}=-\int_0^\infty \frac{F_m}{m|D'|}\exp\left(\frac{-k^3\alpha}{3m|D'|}+ikx\mu\right)dK \tag{13}$$

where

$$F=\frac{\partial\Psi_m}{\partial r}+\frac{2\Omega\Psi_m}{r(\Omega-\omega)}$$

and

$$\alpha=\frac{7\nu}{3}+\xi-\frac{ic^2}{(\Omega-\omega)\,m}. \tag{14}$$

It is easily seen from equation (13) that across the resonance, x changes sign and the major axis of the orbit undergoes a 90° rotation. Furthermore, the resonant effect is significant over $|x|\sim(\alpha/|D'|)^{1/3}\sim\mathcal{R}^{-1/3}r$.

This dependence implies that even a fairly weak viscous force can smear out the resonant zone over a significant region.

The rate of angular momentum transport over the entire resonant zone is

$$\dot{H}=\frac{\pi^2\Sigma r|F|^2}{m(\Omega-\omega)|D'|}\sim q^2H\Omega \tag{15}$$

where

$$F=\frac{\partial\Psi_m}{\partial r}+\frac{2\Omega\Psi_m}{r(\Omega-\omega)}. \tag{16}$$

$\dot{H}$ deduced here is independent of the magnitude of viscosity. The $\dot{H}$ obtained here is identical to that deduced for the resonant angular momentum transport of a self-gravitating but non-viscous disc in the context of Saturn's rings (Goldreich & Tremaine 1978a) and of a gas disc in the context of spiral galaxies (Donner, private communication; Goldreich & Tremaine 1978b). This agreement arises because the tidal torque transports angular momentum at the resonance by exciting a negative angular momentum wave. This wave is then propagated away from the resonant zone and carries angular momentum with it. Such transport does not involve mass movement and is called lorry transport (Lynden-Bell & Kalnajs 1972). The amount of negative angular momentum excited at the resonance is entirely determined by the strength of the tide. Therefore, the amount of negative angular momentum dumped into the fluid is independent of the detailed physics put in provided the negative angular momentum wave will eventually be dissipated either by a viscous effect (in a viscous disc) or by a non-linear effect (in a self-gravitating disc). However, the width of the resonant zone may be quite sensitive to the detailed dissipation mechanism.

In this regard we note that in the centre of the resonance, the perturbed radial velocity is the order of $\mathscr{R}^{1/3}\psi_m/r\Omega$ while ρ'/ρ is of the order of $\Psi'/(r\Omega)^2\,\mathscr{R}^{2/3} \sim q\mathscr{R}^{2/3}$. From this we see that if the local Reynolds number is larger than $q^{-3/2}$, the flow becomes non-linear. This means that the local Reynolds number may adjust to the value $q^{-3/2}$ and the local sound speed increases, leading to a thickness $rq^{1/2}$, rather than $r(\mathscr{R})^{-1/3}$.

From (15), we see that if the basic Reynolds number of the disc is $<q^{-2}$, the viscous process transports angular momentum more efficiently than the resonance effect. In this case the spiral dissipation pattern would be rather open and diffuse, and the resonance would have little effect on the overall dynamics of the disc; on the other hand if the basic Reynolds number is $>q^{-2}$, the resonance plays an important role in the overall dynamics and the disc may even be terminated there.

We are indebted to Drs Goldreich and Tremaine for pointing out to us that the result obtained in Section 2 from scattering considerations can also be deduced by summing up

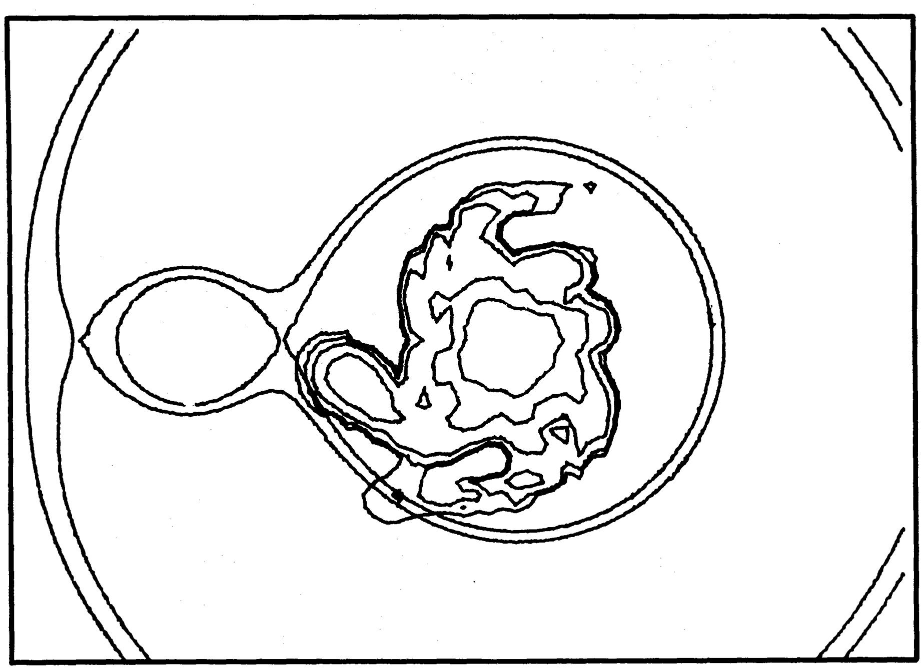

Figure 2. The dissipation pattern of accretion disc flow with mass transfer with $q = 0.1$. The contours are drawn in steps three times their lower contours. A hot spot superimposed on to the spiral pattern is shown.

effects of resonances from $m = 1$ to $m \sim q^{-1/3}$ (which is equivalent to choosing a minimum impact parameter equal to the Roche radius of the secondary). Also the angular momentum flux is reduced below that given by (15) for $m \gtrsim r\Omega/c_s$, accordingly the angular momentum loss from the disc would be less than that estimated in Section 2 for $q^{1/3} < c_s/\Omega r$.

In order to investigate the overall resonant effect on an accretion disc in close binary systems, we performed some numerical simulations. The first series of simulations was the same as that presented in Table 1. In these cases mass transfer from the secondary to the primary via the inner Lagrangian point was switched on at some time and kept at a constant

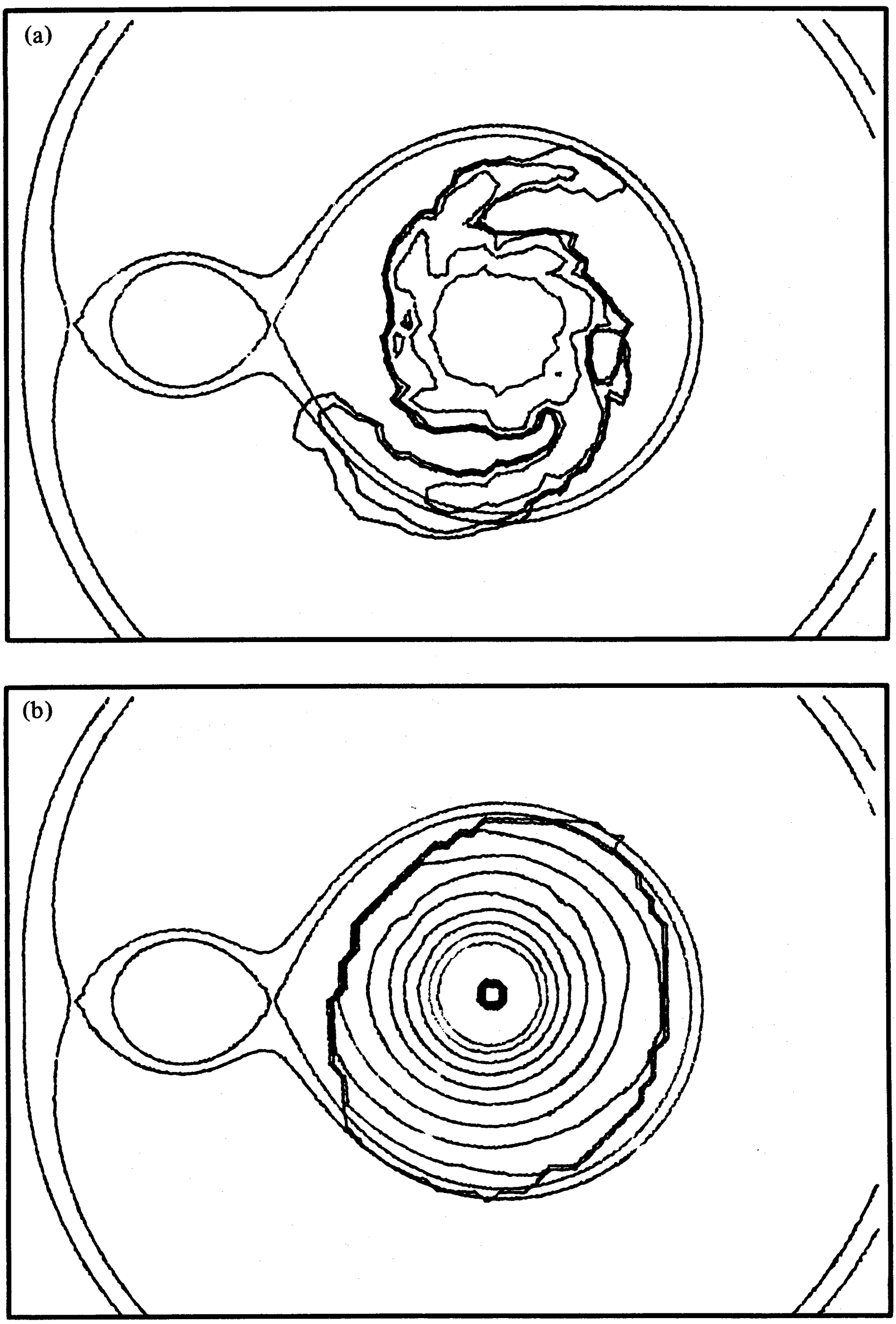

Figure 3. (a) The dissipation pattern of the accretion disc flow with mass transfer switched off, $q = 0.1$. A clear spiral pattern is seen. (b) Contour of circular velocity around the primary. A sharp increase in the shear around the 2 : 1 resonance is shown.

rate. The simulation continued for 20 orbital periods until a steady state was achieved. The dissipation patterns for $q = 0.1$ were then analysed and presented in Fig. 2.

In the dissipation pattern, a hot spot in the region where the stream impacts the disc is easily visible. Such a hot spot is also found in our previous simulations for q of order unity (Lin & Pringle 1976). This hot spot is produced by the shock which the stream experiences upon its impact on to the disc. In many dwarf novae systems, this hot spot may be responsible for a hump in the light curve (see review by Warner 1976). In addition to the normal hot spot, a spiral dissipation pattern can also be found. This spiral pattern extends around

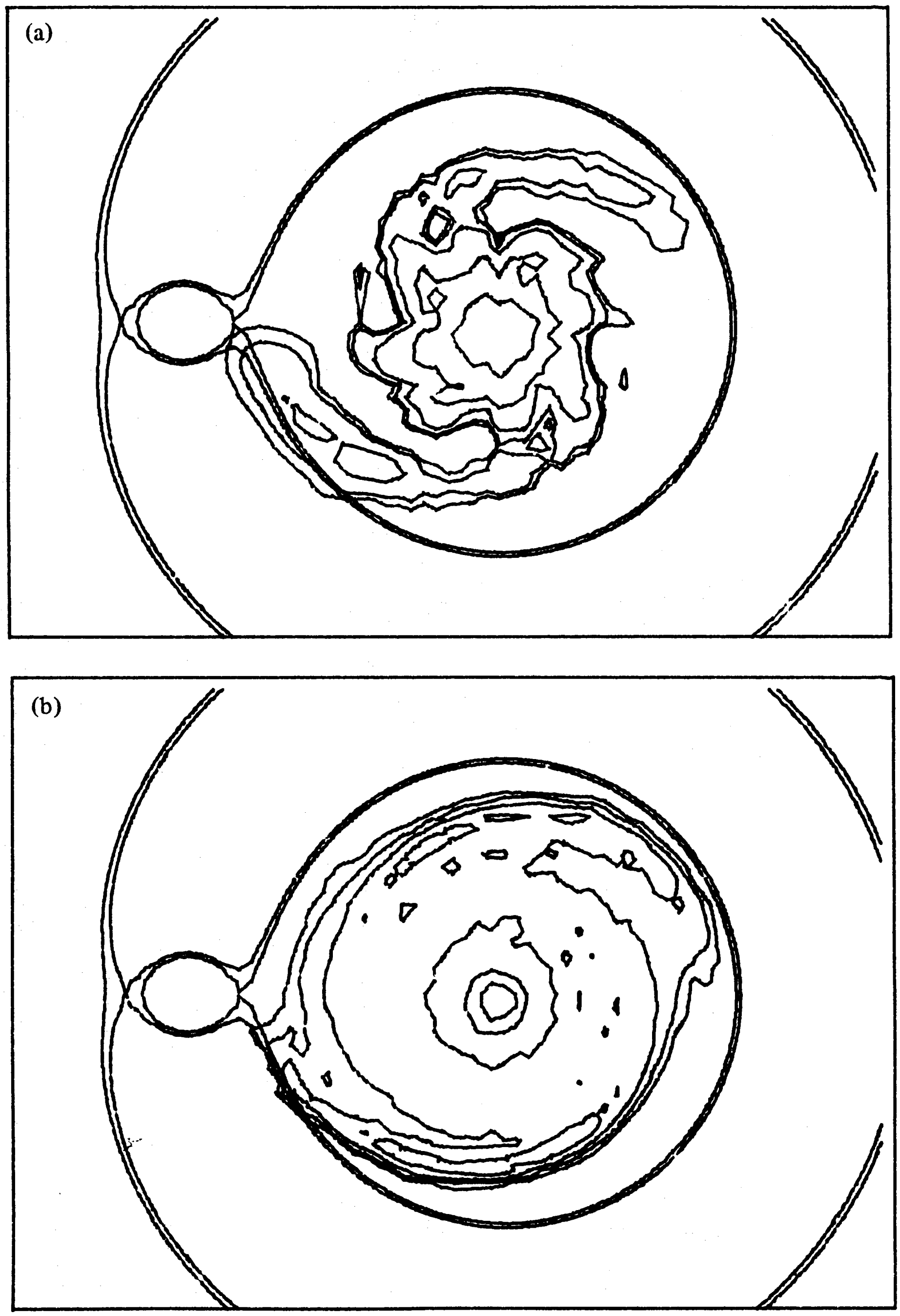

Figure 4. (a) The dissipation pattern of accretion disc flow with mass transfer switched off, $q = 0.02$. The spiral pattern extends from inside the 2:1 resonance to the edge of the Roche lobe. (b) The density contour of a weak spiral pattern is shown.

the 2:1 resonance over about $0.1R$ in the radial direction. Since the magnitude of the Reynolds number chosen is of order a few hundred, this radial spread is in good agreement with our previous analytic estimate.

We continued our simulation for several more orbital periods with the mass transfer switched off. The hot spot disappeared due to the absence of the stream. A prominent spiral pattern dissipation that extends from inside the Lindblad resonance all the way to the edge of the Roche lobe can be clearly seen (see Figs 3 and 4). A similar but less pronounced spiral pattern can also be seen in the density contours. A rapid rise in the circular velocity around the primary near the spiral dissipation region can also be seen. It is this rapid increase in the shear rather than the density which produces the spiral dissipation pattern. These 'clean' simulations are a better representation of our earlier analytic results.

We note that the spiral dissipation generated in our simulation is very similar to those simulated for bar-driven spiral galaxies (Sanders & Huntley 1977; Sanders 1977). This similarity arises because the forcing potentials have the same variation. The width of the spiral arm simulated for the galactic cases also agreed well with our analytic estimates.

4 Observational consequences

Since the spiral pattern only appears for systems with small q, and the width of spiral pattern depends on the magnitude of viscosity, direct observations of the spiral pattern can help us to understand some aspects of the dynamical structure of the disc.

In order to predict an expected light curve, the detailed radiation mechanism must be investigated. However, in the outer region of the disc the structure is neither homogenous nor axisymmetric even on a scale small compared with the radius of the disc. Furthermore, both Kelvin–Helmholtz and convective instabilities are expected to occur near the region of the disc being impinged by the stream. In addition, bolometric corrections may be important in interpreting the observed light curve (Bath *et al.* 1974). All these complications can cast doubts on any simple observational interpretation.

In the light curves of many dwarf novae, hot spots can be observed. These hot spots are generally thought to be produced by the energy released during the impact of the stream on the disc (Warner 1976). As well as these hot spots there may be additional humps in the light curve caused by the spiral dissipation pattern.

Although most dwarf novae have only one hump in their light curve, it has been brought to our attention by Dr J. Faulkner that one particular system, WZ Sge, has two humps in its light curve. It may be significant that WZ Sge is one of the few systems with a mass ratio small enough to produce a spiral dissipation pattern (Robinson, Nather & Patterson 1978; Fabian *et al.* 1978). A detailed model of this type for WZ Sge is in preparation and will be presented elsewhere.

Acknowledgments

We thank Drs Donner, Faulkner, Goldreich, Pringle and Tremaine and Professor Lynden-Bell for useful conversations and the Cambridge University Computer Centre for assistance. DNCL acknowledges a research Fellowship from Trinity Hall.

References

Bath, G. T., Evans, W. D., Papaloizou, J. & Pringle, J. E., 1974. *Mon. Not. R. astr. Soc.*, **169**, 447.

Fabian, A. C., Lin, D. N. C., Papaloizou, J., Pringle, J. E. & Whelan, J. A. J., 1978. *Mon. Not. R. astr. Soc.*, **184**, 835.

Goldreich, P. & Tremaine, S., 1978a. *Icarus*, **34**, 240.
Goldreich, P. & Tremaine, S., 1978b. *Astrophys. J.*, **222**, 850.
Lin, D. N. C. & Pringle, J. E., 1976. *Structure and Evolution of Binary Systems*, p. 257, eds Eggleton, P. P., Mitton, S. & Whelan, J. A. J., D. Reidel, Dordrecht, Holland.
Lynden-Bell, D., 1975. *La Dynamique des Galaxies Spirales*, p. 91, ed. Weliachew, L., CNRS, Paris.
Lynden-Bell, D. & Kalnajs, A. J., 1972. *Mon. Not. R. astr. Soc.*, **157**, 1.
Lynden-Bell, D. & Pringle, J. E., 1974. *Mon. Not. R. astr. Soc.*, **168**, 603.
Papaloizou, J. & Pringle, J. E., 1977. *Mon. Not. R. astr. Soc.*, **181**, 441.
Pringle, J. E. & Rees, M. J., 1972. *Astr. Astrophys.*, **21**, 1.
Robinson, E. L., Nather, R. E. & Patterson, J., 1978. *Astrophys. J.*, **219**, 168.
Sanders, R. H., 1977. *Astrophys. J.*, **217**, 916.
Sanders, R. H. & Huntley, J. M., 1977. *Astrophys. J.*, **209**, 53.
Warner, B., 1976. *Structure and Evolution of Binary Stars*, p. 85, eds Eggleton, P. P., Mitton, S. & Whelan, J. A. J., D. Reidel, Dordrecht, Holland.

Appendix A

In Section 2 we estimated the angular momentum transported to the secondary from a particle initially in a circular orbit from a simple scattering calculation. However, it is of interest to see how the same result follows from a perturbed orbit calculation taking the primary into account. For our coordinate system we use cylindrical polar coordinates based on the primary. We consider a particle which, in the absence of the secondary would be in a circular orbit of radius $r = r_0$, with angular frequency Ω. We define the line $\theta = 0$ as the line joining the primary to the secondary at the instant $t = 0$ at which the three bodies would be aligned if the particle described an unperturbed circular orbit. The equations of motion are then

$$\frac{d^2r}{dt^2} - r\left(\frac{d\theta}{dt}\right)^2 = -\frac{\partial U}{\partial r} \tag{A1}$$

$$r^2\frac{d^2\theta}{dt^2} + 2\frac{dr}{dt}\frac{d\theta}{dt}r = -\frac{\partial U}{\partial \theta} \tag{A2}$$

where the potential

$$U = U_0 + \bar{U}, \tag{A3}$$

and

$$U_0 = -GM/r, \tag{A4}$$

$$\bar{U} = \frac{-Gm_2}{\sqrt{R^2 + r^2 - 2Rr\cos(\theta - \omega t)}} + \frac{Gm_2 rR\cos(\theta - \omega t)}{R^3}. \tag{A5}$$

Treating $\bar{U}$ as small and perturbing the equations of motion, writing

$$r = r_0 + \delta, \quad \theta = \Omega t + \alpha, \tag{A6}$$

we obtain

$$\ddot{\delta} - \delta\Omega^2 - 2r_0\Omega\dot{\alpha} = -\frac{\partial \bar{U}}{\partial r} - \left(\frac{\partial^2 U_0}{\partial r^2}\right)_{r_0}\delta \tag{A7}$$

$$r_0^2\ddot{\alpha} + 2\Omega r_0\dot{\delta} = \frac{\partial \bar{U}}{\partial t}\frac{1}{(\omega - \Omega)}. \tag{A8}$$

We consider the angular momentum transferred to the secondary, while the particle passes from $\theta = -\pi/2 + \omega t$ to $\theta = \pi/2 + \omega t$ for $-\pi/2(\Omega - \omega) < t < \pi/2(\Omega - \omega)$. At the beginning of this interval we take, $\alpha = \alpha = \delta = \dot{\delta} = 0$ and we consider $\bar{U}$ to be negligible at this point.

Thus we obtain

$$r_0^2 \dot{\alpha} + 2\Omega r_0 \delta = \bar{U}/(\omega - \Omega) \tag{A9}$$

$$\ddot{\delta} + \Omega^2 \delta = -\left(\frac{\partial \bar{U}}{\partial r}\right)_{r_0} + \frac{2\bar{U}\Omega}{r_0(\omega - \Omega)} = S. \tag{A10}$$

Now we may write

$$S = \sum_{n=0}^{\infty} a_n \cos\,[n(\omega - \Omega)\,t]. \tag{A11}$$

The solution for δ is then

$$\delta = \sum_{n=0}^{\infty} \frac{a_n[\cos n(\omega - \Omega)\,t - A_n \cos(\Omega t + \epsilon_n)]}{[\Omega^2 - n^2(\omega - \Omega)^2]} \tag{A12}$$

where

$$\epsilon_n = \frac{\pi\Omega}{2(\Omega - \omega)} + \frac{n\pi}{2}$$

and

$$A_n = 1\ (n \text{ even}), \quad A_n = -\frac{n(\Omega - \omega)}{\Omega}\ (n \text{ odd}).$$

The angular momentum transferred to the secondary is $-H$ where

$$H = -\int_{-\pi/2(\Omega-\omega)}^{\pi/2(\Omega-\omega)} \left(\frac{\partial \bar{U}}{\partial \theta}\right) dt. \tag{A13}$$

This may be written alternatively correct to second order as

$$H = \int_{-\pi/2(\Omega-\omega)}^{\pi/2(\Omega-\omega)} \left[\frac{-\bar{U}\ddot{\alpha}}{(\Omega - \omega)^2} + \left(\frac{\partial \bar{U}}{\partial r}\right)_{r_0} \frac{\dot{\delta}}{(\Omega - \omega)}\right] dt \tag{A14}$$

or

$$H = \int_{-\pi/2(\Omega-\omega)}^{\pi/2(\Omega-\omega)} \left\{\dot{\delta}\left[\frac{1}{(\Omega - \omega)}\frac{\partial \bar{U}}{\partial r} + \frac{2\Omega\bar{U}}{r_0(\Omega - \omega)^2}\right] - \frac{\bar{U}}{r_0^2}\frac{\partial \bar{U}}{\partial t}\frac{1}{(\omega - \Omega)}\right\} dt. \tag{A15}$$

As the last term in the brackets integrates to zero, this can be written

$$H = \int_{-\pi/2(\Omega-\omega)}^{\pi/2(\Omega-\omega)} \frac{\dot{\delta} S\, dt}{(\omega - \Omega)} \tag{A16}$$

so

$$H = \sum_{n,m} \int_{-\pi/2(\Omega-\omega)}^{\pi/2(\Omega-\omega)} \frac{a_n a_m \cos\,[n(\omega - \Omega)\,t]\, Q_m\, dt}{[\Omega^2 - m^2(\Omega - \omega)^2](\Omega - \omega)}, \tag{A17}$$

where

$$Q_m = A_m \Omega \sin(\Omega t + \epsilon_m) - (\Omega - \omega)\, m \sin\,[m(\Omega - \omega)\,t]$$

so

$$H = -\sum_{n,m} \frac{4\Omega^2 a_m a_n A_m A_n \sin\epsilon_m \sin\epsilon_m}{\{\Omega^2 - m^2(\Omega-\omega)^2\}\{\Omega^2 - n^2(\Omega-\omega)^2\}(\Omega-\omega)} \tag{A18}$$

or,

$$H = \frac{-1}{(\Omega-\omega)}\left(\sum_n \frac{2\Omega a_n A_n \sin\epsilon_n}{[\Omega^2 - n^2(\omega-\Omega)^2]}\right)^2 \tag{A19}$$

for $\Omega > \omega$, this corresponds to a transfer to the secondary. To estimate the sum, we note that, on the orbit, the maximum of $\bar{U}$ is about Gm_2/r_L, and its scale of variation is r_L.

Accordingly, values of n will be important up to

$$n \sim R/r_L \sim \Omega/(\Omega-\omega). \tag{A20}$$

For such values of n,

$$|a_n| \sim \left|\frac{\partial\bar{U}}{\partial r}\right|\frac{1}{n} \sim \frac{Gm_2}{r_L^2}\frac{r_L}{R}. \tag{A21}$$

The major contribution to the sum comes from a few values of n near the minimum of $|\Omega - n(\Omega-\omega)|$. If $\Omega = n(\Omega-\omega)$ exactly, then

$$\frac{2\Omega\sin\epsilon_n}{\Omega^2 - n^2(\Omega-\omega)^2} = \frac{(-1)^n\pi}{2(\omega-\Omega)}. \tag{A22}$$

We thus estimate H to be

$$H = \frac{\pi^2}{4(\omega-\Omega)^3}\frac{(Gm_2)^2}{R^2 r_L^2} \tag{A23}$$

in good agreement with Section 2 (see equation (3)).

Therefore we are led to the condition $q \gtrsim \mathscr{R}^{-1}$ for the disc to be tidally controlled as before.

Appendix B

Following the treatment initiated in Section 3, we are looking for a thin viscously controlled layer in the vicinity of the resonance, we retain only the terms with the highest radial derivatives in $F_{\nu r}$ and $F_{\nu\theta}$, these are

$$F_{\nu r} = \left(\frac{4\nu}{3} + \xi\right)\frac{d^2 u'_{rm}}{dr^2} \tag{B1}$$

$$F_{\nu\theta} = \nu\frac{d^2 u'_{\theta m}}{dr^2} \tag{B2}$$

where ν and ξ are the shear and bulk viscosities respectively. We remark that including the zero-order radial drift would result in terms with lower order derivatives and, accordingly, this may be neglected.

The perturbed density ρ', satisfies,

$$m\rho'(\Omega-\omega) = -\rho\,\nabla\cdot\mathbf{u}' \tag{B3}$$

and the perturbed pressure satisfies $p' = \rho' c^2$ where c is the isothermal sound speed.

Substituting the above into the equations of motion, we find (keeping only higher-order radial derivatives),

$$i(\Omega-\omega)\,mu'_{rm}-2\Omega u'_{\theta m}=\left[\frac{4\nu}{3}+\xi-\frac{c^2 i}{m(\Omega-\omega)}\right]\frac{d^2u'_{rm}}{dr^2}-\frac{\partial\Psi'_m}{\partial r} \tag{B4}$$

$$i(\Omega-\omega)\,mu'_{\theta m}+\frac{u'_{rm}\Omega}{2}=\nu\frac{d^2u'_{\theta m}}{dr^2}. \tag{B5}$$

The strongly viscous case arises when

$$\left(\frac{4\nu}{3}+\xi\right)\gtrsim\frac{c^2}{\Omega}$$

or equivalently when

$$\frac{R^2\Omega^2}{c^2}\gtrsim\mathscr{R}.$$

This is the case for most accretion disc models (Pringle & Rees 1972).

Combining the equations of motion, we obtain

$$u_{rm}\left[im(\Omega-\omega)+\frac{\Omega^2}{im(\Omega-\omega)}\right]+\frac{\partial\Psi'_m}{\partial r}+\frac{2\Omega\Psi'_m}{r(\Omega-\omega)}$$
$$=\left(\frac{4\nu}{3}+\xi-\frac{c^2 i}{m(\Omega-\omega)}\right)\frac{d^2u'_{rm}}{dr^2}+\frac{2\Omega\nu}{im(\Omega-\omega)}\frac{d^2u'_{\theta m}}{dr^2}. \tag{B6}$$

Now at the resonance, where $r=r_s$

$$m^2(\Omega-\omega)^2=\Omega^2.$$

This means that the coefficient of u_{rm} is proportional to x, where $x=r-r_s$. We therefore anticipate that the width of the resonance region will be given by

$$\Delta x\sim r\left(\frac{\nu}{\Omega r_s^2}\right)^{1/3}\sim r\mathscr{R}^{-1/3}.$$

From (B5) it follows that

$$i(\Omega-\omega)\,m\frac{d^2u'_{\theta m}}{dr^2}=-\frac{\Omega}{2}\frac{du'_{rm}}{dr^2}+0(\nu^{-1/3}).$$

Combining this with (B6), we obtain

$$u'_{rm}\left[im(\Omega-\omega)+\frac{\Omega^2}{im(\Omega-\omega)}\right]+\frac{\partial\Psi'_m}{\partial r}+\frac{2\Omega\Psi'_m}{r(\Omega-\omega)}$$
$$=\left[\nu\left(\frac{4}{3}+\frac{\Omega^2}{m^2(\Omega-\omega)^2}\right)+\xi-\frac{c^2 i}{m(\Omega-\omega)}\right]\frac{d^2u'_{rm}}{dr^2}. \tag{B7}$$

We consider (B7) near the resonance, by transforming from r to x, and writing

$$im(\Omega-\omega)+\frac{\Omega^2}{im(\Omega-\omega)}=imD'x.$$

We then obtain

$$imu'_{rm}D'x + F = \alpha \frac{d^2u'_{rm}}{dr^2} \tag{B8}$$

where

$$F = \frac{\partial\Psi'_m}{\partial r} + \frac{\partial\Omega\Psi'_m}{r(\Omega-\omega)}, \quad \alpha = \frac{7\nu}{3} + \xi - \frac{ic^2}{(\Omega-\omega)}.$$

If we treat the coefficients and F as constants in (B8), we can write the solution as a Fourier integral in the form

$$u'_{rm} = -\int_0^\infty \frac{F\exp[-(k^3\alpha/3m|D'|) + ikx\mu]}{m|D'|}\,dk, \tag{B9}$$

where

$\mu = D'/|D'|$.

We now calculate the angular momentum loss in the disc. This is

$$\dot{H} = \int_{-\infty}^{\infty}\int_0^{2\pi} \mathrm{Re}[\rho']\,\mathrm{Re}[im\Psi'_m]\; r\,d\theta\,dr\,dz$$

or

$$\dot{H} = \int_{-\infty}^{\infty}\int_0^{2\pi} \frac{1}{m}\,\mathrm{Re}\left\{\frac{\rho i}{(\Omega-\omega)}\left[\frac{\partial ru'_{rm}}{\partial r} + \frac{imu'_{\theta m}}{r}\right]\right\}\mathrm{Re}[im\Psi'_m]\,r_s\,d\theta\,dx\,dz.$$

After doing an integration by parts and using (B5), we obtain

$$\dot{H} = -\int_{-\infty}^{\infty}\int_0^{2\pi} \frac{r_s\,d\theta\,dx\,\Sigma\,\mathrm{Re}(iu_{rm})\,\mathrm{Re}(imF)}{(\Omega-\omega)\,m}$$

$$\dot{H} = \int_{-\infty}^{\infty}\int_0^{2\pi} \frac{r_s\Sigma\,\mathrm{Re}(imF)}{m(\Omega-\omega)}\int_0^\infty \exp(-\alpha k^3/3m|D'|)\,\mathrm{Re}\left[\frac{iF\exp(ik\mu x)}{m|D'|}\right]dk\,d\theta\,dx$$

$$\dot{H} = \frac{\pi^2\Sigma r_s|F|^2}{m(\Omega-\omega)|D'|} \tag{B10}$$

which is the same as Goldreich & Tremaine (1977).

The result as we see is completely independent of the viscosity and it can even be obtained by ignoring all physics and merely adding a small positive imaginary part to ω. It gives $\dot{H} \sim q^2\Omega H_{\mathrm{disc}}$ and thus cannot be significant for an accretion disc unless $\mathscr{R} > q^{-2}$. Thus for $q^{-1} < \mathscr{R} < q^{-2}$, it is possible for the disc to be tidally limited but not to feel the effect of the resonance. For $\mathscr{R} > q^{-2}$ it is possible for the disc to be truncated at the resonance rather than the Roche lobe.